BIOCHEMISTRY

 Volume 46, Number 19 May 15, 2007

Articles

Properties of Nucleosomes in Acetylated Mouse Mammary Tumor Virus versus 5S Arrays†

F. J. Solis,[‡,§] R. Bash,[‡,||,⊥,#] H. Wang,[‡,||,#] J. Yodh,[△,○] S. A. Lindsay,[||,#] and D. Lohr*[,⊥]

Department of Integrated Natural Life Sciences, Arizona State University West, Glendale, Arizona 85306, Department of Physics and Astronomy, Department of Chemistry and Biochemistry, and Biodesign Institute, Arizona State University, Tempe, Arizona 85287, and Division of Basic Sciences, Arizona College of Osteopathic Medicine, Midwestern University, Glendale, Arizona 85308

Received October 10, 2006; Revised Manuscript Received February 5, 2007

ABSTRACT: Acetylation is one of the most abundant histone modifications found in nucleosomes. Although such modifications are thought to function mainly in recognition, acetylation is known to produce nucleosome structural alterations. These could be of functional significance in vivo. Here, the basic features of mouse mammary tumor virus (MMTV) promoter nucleosomal arrays reconstituted with highly acetylated histones prepared from butyrate-treated HeLa cells are characterized by atomic force microscopy. Results are compared to previous results obtained with hypoacetylated MMTV and hyper- or hypoacetylated 5S rDNA arrays. MMTV arrays containing highly acetylated histones show diminished intramolecular compaction compared to hypoacetylated MMTV arrays and no tendency for cooperativity in nucleosome occupation. Both features have been suggested to reflect histone tail-mediated internucleosomal interactions; these observations are consistent with that suggestion. 5S arrays show qualitatively similar behavior. Two other effects of acetylation show stronger DNA template dependence. Nucleosome salt stability is diminished in highly acetylated compared to hypoacetylated MMTV arrays, but nucleosome (histone) loading tendencies are unaffected by acetylation. However, highly acetylated histones show reduced loading tendencies on 5S templates (vs hypoacetylated), but 5S nucleosome salt stabilities are unaffected by acetylation. ATP-dependent nucleosome remodeling by human Swi-Snf is similar on hyper- and hypoacetylated MMTV arrays.

Chromosome structure plays a critical role in the processes of replication, transcription, and repair in eukaryotes, and the past 10 years or so has seen tremendous progress in understanding the basic elements of this structure, nucleosomes and arrays of nucleosomes (*1*−*9*). Nucleosomal arrays are the foundation of in vivo chromosome organization. Studies of their intrinsic properties provide important insights into this fundamental organization, including information about nucleosome structure that cannot be obtained from studies of mononucleosomes (*6*, *10*, *11*).

Nucleosomal arrays reconstituted on the concatameric 5S rDNA templates developed by Simpson and co-workers (*12*) are widely used for in vitro chromatin studies. These arrays can be reconstituted, at both saturated and subsaturated loading levels, into defined structures suitable for biophysical

† Grant support to R.B., H.W., S.A.L., and D.L. (NIH, CA-85990) is gratefully acknowledged.

* To whom correspondence should be addressed. Fax: 480-965-2747. Phone: 480-965-5020. E-mail: dlohr@asu.edu.

‡ These authors contributed equally to this work.

§ Arizona State University West.

|| Department of Physics and Astronomy, Arizona State University.

⊥ Department of Chemistry and Biochemistry, Arizona State University.

Biodesign Institute, Arizona State University.

△ Midwestern University.

○ Current address: School of Molecular and Cellular Biology, University of Illinois at Urbana−Champaign, Urbana, IL 61801.

10.1021/bi062116z CCC: $37.00
Published on Web 04/20/2007

and biochemical studies (*6*, *13*). The individual 5S units preferentially position nucleosomes (*14*, *15*), and histone assembly order resembles that in vivo (*16*). These arrays provide a very tractable system. However, their repetitive nature differs from most in vivo nucleosomal arrays.

We have used atomic force microscopy (AFM) to study the basic features of nucleosome occupation on both 208-12 (*17*−*19*) and 172-12 (*19*, *20*) 5S arrays. AFM is a powerful imaging technique for studies of nucleic acids and nucleoprotein complexes (*21*−*23*), and the technique has major advantages for chromatin studies. Single molecule resolution provides precise distributions for specific array features, such as numbers of nucleosomes or internucleosomal distances (*17*−*20*, *24*−*28*). Modeling approaches can be applied to that data, for quantifiable insights (*19*). Subsaturated arrays are typically used in these types of studies because of the occupancy choices available on such templates, which can reveal unique information about fundamental features of occupation, and because quantitative analyses are less ambiguous than for saturated arrays, which tend to compact in the AFM (*27*). Subsaturated arrays may serve as models for newly replicated, gene promoter (*29*) and replication origin (*30*, *31*) chromatin, which are often subsaturated.

The ability of AFM to image in solution is particularly useful. This feature allows imaging of chromatin to take place in an aqueous (physiologically relevant) environment and presents the opportunity to alter that environment in order to study either intrinsic features, such as nucleosome salt stability (*26*, *27*), or chromatin-associated processes, such as ATP-dependent nucleosome remodeling (*32*−*34*), at the level of individual array molecules. The ability to identify specific types of molecules in solution AFM images (*33*−*35*) will further enhance the usefulness of AFM for studies of chromatin and the changes it undergoes.

Concerns about the unphysiological nature of repetitive templates like the 5S led us to undertake AFM studies of a single copy DNA template, ∼1.9 kb in length, containing the MMTV (mouse mammary tumor virus) promoter region (*26*, *27*, *32*−*35*). The MMTV promoter has long been a premier model for nucleosome structure and structural changes in response to gene activation, both in vivo (*36*, *37*) and in vitro (*38*, *39*). Studying salt-reconstituted, single copy templates can be problematic using traditional approaches, but salt-reconstituted (subsaturated) MMTV arrays are as suitable for AFM study as subsaturated 5S arrays (*27*). The properties of subsaturated MMTV and 5S arrays show clear differences when analyzed by AFM approaches, demonstrating that the nature of the DNA template can affect fundamental chromatin features.

In vivo, the histone component of nucleosomes is subject to covalent modifications, on the N-terminal tails that project out from the compact core nucleosome structure (*40*−*47*) as well as within the compact core domain itself (reviewed in ref *48*). Lysine acetylation, one of the most common of these modifications, is known to be extremely important in vivo for both replication (*49*) and transcription (*40*−*48*, *50*−*52*). A major functional role of acetylation, and other modifications, involves recognition, marking nucleosomes for interaction with specific factors or targeting them for further modification. However, the presence of acetylated histones does alter the structural properties of nucleosomes and nucleosomal arrays (reviewed in refs *3* and *4*). For example, acetylation seems to "loosen" the DNA−histone interaction in individual nucleosomes, thus reducing the level of restrained supercoiling and enhancing transcription factor access. Acetylation also affects the higher order structure of chromatin. By decreasing the extent of internucleosomal contact, acetylation diminishes the folding of nucleosomal arrays (*11*, *53*). In fact, acetylation of a single site on H4, Lys_{16}, was recently shown to be sufficient to cause striking changes in chromatin folding (*54*). Modifications located within the histone core domains are likely to have significant effects on nucleosome stability and perhaps on folding (*48*). The recognition aspects of acetylation have received major attention, but the structural alterations associated with acetylation are also likely to be functionally significant in vivo (*51*).

Here, we characterize the properties of (subsaturated) MMTV nucleosomal arrays reconstituted with highly acetylated histones isolated from butyrate-treated cells and compare these properties to those of hypoacetylated MMTV and highly acetylated or hypoacetylated 5S arrays. The results demonstrate that the presence of highly acetylated histones produces some effects that are similar on MMTV and 5S arrays and some effects that differ; the latter indicate that acetylation effects can be DNA template (sequence) dependent. An analysis of nucleosome remodeling by the ATP-dependent remodeling complex human Swi-Snf finds very similar remodeling changes on highly acetylated and hypoacetylated MMTV arrays.

MATERIALS AND METHODS

Chromatin Reconstitution. 5S (172-12 and 208-12) and MMTV DNA fragments were isolated as described (*17*, *20*, *27*). The ∼1850 bp *Nco*I−*Sph*I MMTV fragment contains 400 bp of CAT DNA and 1500 bp of viral sequence, including the entire MMTV promoter region. Histone octamers were prepared as described from butyrate-treated or untreated HeLa cells (*17*, *18*, *20*). Octamers isolated from butyrate-treated cells will be designated as "highly acetylated" or "hyperacetylated" in the work below and octamers from untreated cells as "hypoacetylated", to reflect the fact that they are not completely devoid of acetylation. We estimate (from gels scans) that the average acetylation levels in the highly acetylated histones are 8−10 acetyl groups per octamer, residing mainly in histones H3 and H4 (*18*, *20*). The hypoacetylated histones contain, on average, <1 acetyl group per octamer. Nucleosomal arrays were reconstituted and glutaraldehyde-fixed as described in ref *27*. Reconstituted samples were checked by electrophoresis on native 3.5% polyacrylamide gels. Mobility on these gels depends on nucleosome occupation level, and this assay provides a qualitative check on reconstitution (Bash et al., unpublished results).

Deposition and Imaging of Chromatin. Samples of reconstituted, fixed arrays were deposited on APTES (aminopropyltriethoxysilane) or GD-APTES surfaces, both made as described in ref *26*. Images were taken in air (for template occupation level studies) or in liquid (for template occupation level, internucleosomal distance, salt stability, and remodeling studies). Population (template occupation level) values are the same whether measured in air or in solution (Bash et al., unpublished observations). Images are taken with a

Multi-Mode SPM instrument equipped with an E-scanner (Digital Instruments, Inc., Santa Barbara, CA) for images in air. Noncontact conical sharp silicon tips (NCH; Nanosensor), and Ultrasharp Noncontact silicon cantilevers (NSC 15/50; MikroMasch Inc.) were used for imaging. The typical tapping frequency was 290−340 kHz for the NCH tips and 340−380 kHz for the NSC 15/50 probes; the scanning rate was 2−3 Hz. Solution imaging was carried out with a Macmode PicoSPM (Molecular Imaging, Tempe, Az) equipped with triangular Si_3N_4 cantilevers (Molecular Imaging, Phoenix, AZ) with a spring constant of 0.1 N/m. Measurements were performed at about 8 kHz driving frequency and 5 nm oscillation amplitude. For solution imaging, e.g., for the salt titrations (*26*), the prepared sample is mounted into an SPM liquid flow cell (Molecular Imaging, Phoenix, AZ), and NaCl solutions of increasing concentration are injected into the flow cell in situ and scanned after 10 min with 8% amplitude reduction. The scanning rate was 1.78 Hz.

Determining Nucleosome Numbers and Measuring Nucleosome Locations on the Templates. For each reconstituted sample, nucleosome numbers on at least 150 array molecules were determined. Molecules to be counted had to have distinguishable nucleosomes and discernible template termini. Every acceptable molecule in a field was counted to avoid bias. Each molecule analyzed was marked in order to avoid remeasuring it.

To perform the measurements, AFM images of nucleosomal arrays were converted from nanoscope format (Digital Instruments, Inc.) into TIF files and the measurements made using Scion (NIH Image) software. Distances were measured from a template terminus to the center of the first nucleosome encountered, then progressively to the centers of each successive nucleosome, and finally from the center of the terminal nucleosome to the adjacent template terminus (*19*). The data were sorted as distances from a template terminus ("end distances") and as distances between nucleosome centers ("internucleosomal distances"). The data were initially sorted by n, the number of nucleosomes on a template, and compiled (summing over all n) as needed. As an internal check, contour lengths for each molecule were also recorded. The contour length varies slightly among molecules but decreases consistently as the number of nucleosomes present on the molecule increases, as expected.

Analysis of Population and Distance Data for Chromatin Arrays. Previously, we presented a theoretical framework for analyzing nucleosome population and distance data from the AFM in order to quantify nucleosome occupational features (*19*). Data from studies of 208-12 (and some 172-12) 5S rDNA arrays were analyzed in that work. The method assumes that interactions between nucleosomes and between the DNA template and histones can be treated as small deviations from a random occupation model. The approach can be applied to any AFM data, and here we extend it to MMTV promoter arrays.

The model allows the determination of several quantities describing various nucleosomal array features. DNA−histone association constants can be determined from population distributions, that is, from the statistical distributions of the numbers of nucleosomes on arrays, at various DNA and histone concentrations. Using the model, the experimental population distribution can be fitted to a theoretical distribution that depends on a parameter, w, and several constants including the length of DNA wrapped around the nucleosome. The parameter w is the difference between the chemical potential of the histone octamer in solution, μ, and the formation energy of a nucleosome, g, i.e., $w = (g - \mu)/kT$ (k is the Boltzmann constant and T the temperature). If the chemical potential of octamers is due only to their solution entropy, its value is equal to the logarithm of the octamer concentration [H], $\mu = \ln [H]$. Regression fits of the values of w with respect to the logarithm of the octamer concentration lead to a determination of the association constant for the nucleosome as $K = [H]_o^{-1}$, where $[H]_o$ is the histone octamer concentration that makes the value of the w parameter equal to zero. This association constant refers to the association of a segment of DNA of a nominal length L with a histone octamer; i.e., L is the length of DNA in the nucleosome. We use average L values determined from analysis of array contour lengths and nucleosome numbers. We note that the average values we determine are typically less than what is considered to be the canonical core nucleosome length of 147 bp. Evidence for shorter wrap lengths has been reported (reviewed in ref *55*), and we will present AFM data in support of shorter lengths elsewhere (Solis et al., in preparation). Note that the L value affects the absolute magnitude of model-derived quantities, but relative differences (between any two cases) are not highly sensitive to the value of L so long as the same value is used for the two cases being compared. For example, the choice of L value affects the absolute magnitude of association constants for highly acetylated or hypoacetylated 5S arrays but not relative differences between the two (see ref *19*). The various comparisons shown in this work, 5S vs MMTV arrays/highly acetylated vs hypoacetylated, all involve the same L values, ~130 bp. This allows us to make meaningful comparisons of the relative differences in K_a or other quantities.

The distributions of internucleosomal distances on the template provide information on nucleosome−nucleosome interactions. Nearest neighbor nucleosome interactions are best quantified by the use of a virial coefficient. This virial coefficient, v_2, can be interpreted as an effective excess (or deficit) of length created by nucleosome−nucleosome interactions. An enhancement of occupation of the neighboring region to a given nucleosome is equivalent to the creation of an excess length in the random positioning model. We have determined the virial coefficients associated with specific regions within a distance of 35 nm from the center of nucleosomes, in all cases. Assuming a uniform interaction over this region allows the conversion of a virial coefficient into the average interaction energy V_2. The data for population and distance analyses were taken in very low salt, so the values correspond to these conditions. For a complete discussion of the model, please see ref *19*.

Nucleosome Remodeling Studies. The nucleosome remodeling protocol has been described previously (*32*). Briefly, subsaturated chromatin arrays are incubated with the ATP-dependent nucleosome remodeling complex human Swi-Snf (hSwi-Snf) in deposition buffer (10 mM NaCl/5 mM NaH_2PO_4, pH = 7.5) for 25 min and then deposited and imaged in a flow cell linked to the AFM. The sample is scanned twice, to assess the levels of scanning-induced change, then 1 mM ATP (plus Mg^{2+}) is flowed into the sample to activate

hSwi-Snf, and the sample is rescanned after 30 min, to check for remodeling changes. Images were acquired in a scan time of 5 min per image. The hSwi-Snf was a generous gift from G. Hager.

By scanning the same field and thus the same individual array molecules before and after hSwi-Snf activation, it is possible to monitor remodeling changes on individual arrays. It is possible to show that some changes (+ATP vs −ATP) are clearly remodeling-induced as opposed to being instrument-induced (see text and ref *32*). We note that the GD-APTES surface tethers nucleosomes (via the histones) but leaves the nucleosomal DNA as well as some histones relatively free to move (*26*, *32*−*34*).

RESULTS

We previously used AFM approaches to compare the basic features of hypoacetylated MMTV and 5S subsaturated nucleosomal arrays (*27*) as well as highly acetylated and hypoacetylated, subsaturated 5S arrays (*18*−*20*). Here, the same approaches and a statistical mechanical model that can analyze AFM data quantitatively are used to determine the basic features of MMTV arrays reconstituted with highly acetylated histones (see Materials and Methods), for comparison to the previous studies.

Array Compaction Is Mitigated in Highly Acetylated Arrays. Nucleosomes were reconstituted on an ∼1900 bp MMTV promoter DNA fragment (*27*) by a stepwise salt dialysis protocol (*18*−*20*, *26*, *27*), using highly acetylated HeLa histone octamers isolated from butyrate-treated nuclei (*17*, *18*). The average acetylation level of these histones is 8−10 acetyl groups per octamer, residing mainly on histones H3 and H4, whereas the hypoacetylated histones contain on average <1 acetyl group per octamer. Arrays were reconstituted to various levels of subsaturation by varying the input histone levels.

Representative AFM images of highly acetylated and hypoacetylated MMTV arrays are shown in Figure 1. The two types of arrays are very similar in appearance at low to medium levels of nucleosome occupation (cf. Figure 1A vs 1C). However, at higher occupation levels, there are some significant differences (Figure 1B vs 1D). We previously observed (*27*) that as the average occupation level of (hypoacetylated) nucleosomes on the MMTV DNA template approaches ∼8 (these templates should saturate at 12 nucleosomes), images start to show significant numbers of intramolecularly compacted array molecules. At higher input histone levels, such compacted molecules dominate the image (cf. Figure 1D). The presence of highly acetylated histones mitigates this compaction behavior; higher histone inputs are required to observe significant compaction, and even at those occupation levels, compaction is typically less extensive (Figure 1B). For example, acetylated samples at occupation levels as high as $n_{av} \sim 10$ can still contain uncompacted array molecules.

The presence of acetylated histones is known to decrease the levels of nucleosomal array folding in solution (*6*, *51*, *53*, *54*) by reducing the level of internucleosomal contact (*11*). Folding in solution is probably analogous to compaction in the AFM. Thus, an acetylation-induced reduction in array compaction is consistent with solution results and strengthens the suggestion (*27*) that compaction of hypoacetylated

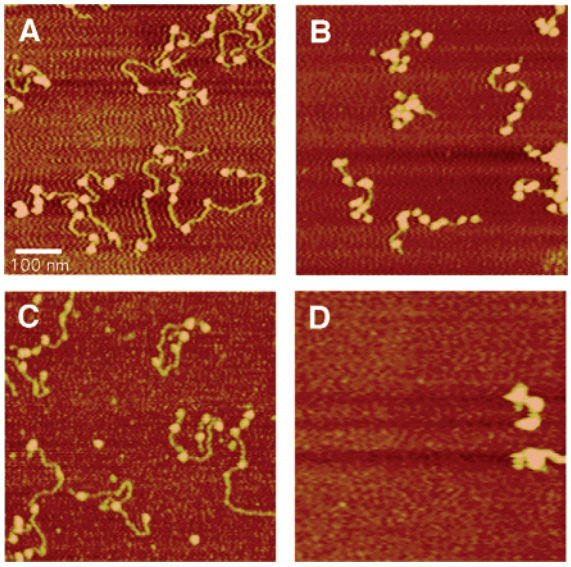

FIGURE 1: AFM images. Images of two highly acetylated MMTV samples (from the same set of reconstitutions; see ref *27*) with different average nucleosome occupation levels, panel A ($n_{av} = 4.7$) and panel B ($n_{av} = 9.5$), and two hypoacetylated samples (from the same set of reconstitutions), panel C ($n_{av} = 4.7$) and panel D (n_{av} indeterminate), are shown. Panel D illustrates the type of sample obtained when using a histone input that would be expected to produce an $n_{av} > 8$ (*27*). These samples contain highly compacted array molecules (their abundance increases with increasing histone imput), and they always have many fewer molecules in the images than samples at lower nucleosome occupation levels, even though they are reconstituted at the same DNA concentration and otherwise treated the same. These images were taken in air; solution images of the same samples show similar results (data not shown).

MMTV arrays in AFM images results from tail-mediated internucleosomal contacts. Surface attachment of arrays in our studies occurs through the histones, probably via the lysine residues in the tails (*26*). Thus, highly acetylated arrays might be less firmly attached to the surface than hypoacetylated arrays, which, in principle, could also affect compaction behavior. Note, however, that we have never observed any direct evidence of less firm surface attachment of these acetylated arrays, for example, when samples are repetitively imaged (*18*−*20*, this work).

Histone Loading Tendencies on MMTV Arrays Are Not Affected by Acetylation. To study the tendencies for nucleosomes (histones) to load on MMTV DNA templates, reconstitutions were carried out at various levels of input histone octamer (DNA levels held constant), and the numbers of nucleosomes present on array molecules (in the types of images shown in Figure 1) were counted to obtain population distributions. A statistical mechanical model presented previously (*19*) can use these data to quantify template loading tendencies. This involves plotting w, a fitted parameter related to the chemical potential of histone octamers, vs ln [H]. [H] is the free octamer concentration in a reconstituted sample (Materials and Methods).

Such data for highly acetylated (filled circles) and hypoacetylated (open circles) histone loading on MMTV DNA templates are shown in Figure 2. The data typically show significant scatter (*19*), due probably to variations inherent in these nucleosome reconstitutions (very small amounts of material, variable adsorption of histones on dialysis tubing, etc.). Nevertheless, it is clear that the results for highly

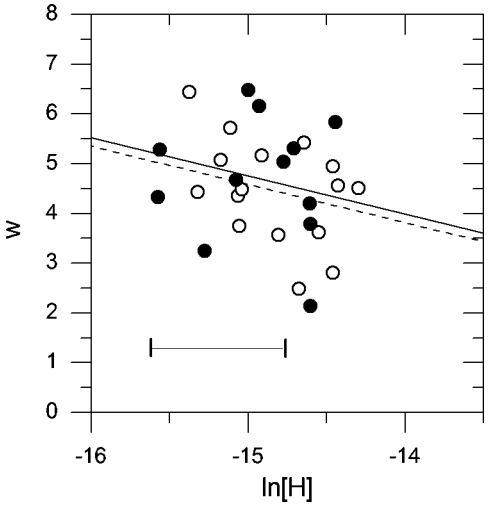

FIGURE 2: Acetylation does not detectably affect MMTV nucleosome (histone) loading preferences. Samples were reconstituted at various levels of input, highly acetylated or hypoacetylated histone (DNA levels held constant), and the numbers of nucleosomes present on MMTV array molecules were counted. Template loading tendencies are quantified from these data by plotting *w*, a fitted parameter related to the chemical potential of free histone octamers, vs ln [H], where [H] is the free octamer concentration (*19*). The filled circles are data for highly acetylated MMTV arrays (fit with a solid line), and the open circles are data for hypoacetylated MMTV arrays (fit with a dotted line). The horizontal bar shows the spread of data in the concentration direction. A DNA wrapping length around the nucleosome of ~130 bp produced the best fit to the data. Uncertainty in the values of the fitted parameter *w* is negligible; the error bar reflects dispersion in the linear regression fits of the *w* parameter vs ln [H].

Table 1: Association Constants[a] (K_a) and $\Delta\Delta G$[b] for Hypoacetylated and Highly Acetylated Nucleosomal Arrays

template	K_a (M^{-1}) hypoacetylated	K_a (M^{-1}) acetylated	$\Delta\Delta G$ (kcal M^{-1})	L[c] (bp)
MMTV	$8 \pm 4 \times 10^3$	$6.5 \pm 3 \times 10^3$	$+0.1 \pm 0.05$	130
5S (208-12)[d]	$120 \pm 60 \times 10^3$	$66 \pm 30 \times 10^3$	$+0.5 \pm 0.2$	127

[a] The equilibrium constant for histone−DNA association, i.e., nucleosome formation. [b] $\Delta\Delta G = \Delta G_{\text{acetylated nucleosome formation}} - \Delta G_{\text{hypoacetylated nucleosome formation}}$. [c] Average wrap length (see Materials and Methods). [d] The 5S data are taken from Table 2 of ref *19*.

acetylated and hypoacetylated MMTV arrays are similar; the data points for the two types of arrays are, on average, coincident. The data fits in Figure 2 provide values for the association constants. These are quite similar (Table 1), corresponding to a $\Delta\Delta G \sim 0.1$ kcal/mol. Such differences are insignificant due to the large uncertainties in these determinations. Thus, by this measure, the use of highly acetylated histones does not detectably affect the thermodynamic tendency for nucleosome (histone) loading on MMTV templates. A simpler analysis, plotting the average number of nucleosomes on arrays (n_{av}) in individual samples reconstituted at various input histone levels, also shows quite similar behavior for hyper- and hypoacetylated MMTV samples (data not shown), in agreement with the above conclusion.

On the other hand, using this same approach, we previously found that loading tendencies for hyper- and hypoacetylated histones on 5S arrays differ. When analyzed as in Figure 2, i.e., plots of *w* vs ln [H], the data points for the two types of 5S arrays (for both 172-12 and 208-12 5S DNA templates) are not coincident (Figure 6 of ref *19*). Analysis using the model finds that association constants for nucleosomes on 5S arrays are reduced roughly 2-fold with acetylated histones (Table 1 of ref *19*). This corresponds to an ~0.5 kcal/mol less favorable ΔG for highly acetylated vs hypoacetylated nucleosome formation on 5S arrays. Also, a plot of n_{av} vs input histone for individual 5S samples shows a reduced loading tendency for highly acetylated histones (*20*). Thus, the effects of histone acetylation on template loading tendencies can vary with the DNA template; i.e., these tendencies can be template-dependent. We have no explanation for this dependence. Other techniques have shown that the optimal octamer concentrations in reconstitutions of mononucleosomes can be sequence-dependent (*56*), which may be another manifestation of the same feature.

The association constants for nucleosome formation on MMTV templates are smaller than those for nucleosomes on 5S templates. The differences are roughly 15-fold for hypoacetylated and ~10-fold for highly acetylated nucleosomes (Table 1). These results show that the average DNA−histone affinity for nucleosomes in MMTV arrays is lower than 5S DNA−histone affinity, as expected (*27*). Note that because the MMTV template is single copy, the association constant values for nucleosomes could vary within the DNA template. Indeed, ensemble-average results suggesting differing DNA−histone affinities for two mononucleosome locations on this template have been presented (*57*). Thus, the MMTV values in Table 1 should be considered an average. Association constants for nucleosomes in 5S arrays, which contain 12 identical repeated units, should be more uniform across the array.

Cooperativity in Nucleosome Occupation Is Abolished in Highly Acetylated Arrays. AFM measurements of nucleosome locations on a large number of arrays (Materials and Methods) can provide information on nucleosome positioning tendencies and information on the influences of internucleosomal interactions in template occupation, i.e., cooperativity in occupation (*18*, *19*).

Subsaturated MMTV arrays, acetylated or not, show no significant nucleosome positioning tendencies in an AFM analysis (data not shown) except for a strong preference for nucleosome occupation at DNA termini. Similar end preferences are observed for 5S arrays (*18*, *19*) and have been known for some time from biochemical studies (*58*). These AFM approaches are capable of detecting nucleosome positioning; positioning is observed on subsaturated 208-12 5S arrays (*18*, *19*). However, even in that case, the degree of positioning determined by AFM is weaker than that inferred from biochemical analyses (*14*), perhaps reflecting the fact that the AFM studies use subsaturated arrays whereas the biochemical analyses use saturated arrays. The latter reduce the randomizing influence of entropy on positioning.

Internucleosomal distance data for 5S nucleosomal arrays detects a cooperative tendency for nucleosome occupation in hypoacetylated arrays that is absent in highly acetylated arrays (*18*, *19*). We find similar behavior for MMTV arrays (Figure 3). Internucleosomal distance plots for hypoacetylated MMTV arrays show a prominent peak at very short distances (Figure 3, upper panel, filled circles). This peak lies well above the random (theoretical) expected level (thick solid line). Such behavior reflects correlated nearest neighbor nucleosome occupation, i.e., cooperativity in occupation (*18*,

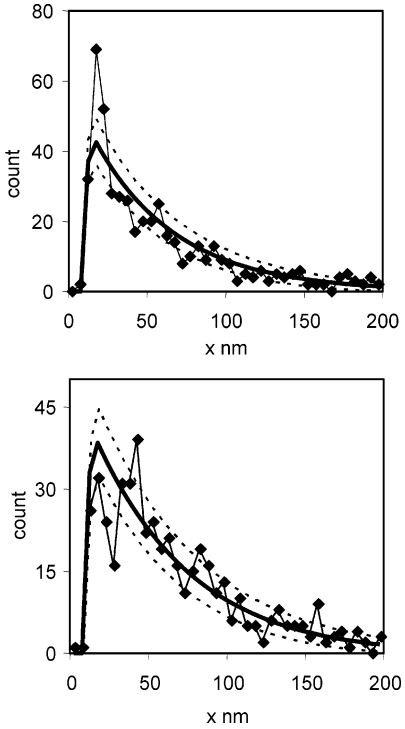

FIGURE 3: Acetylation abolishes cooperative nucleosome occupation of MMTV arrays. Internucleosomal distance distributions, i.e., the numbers of molecules (*y*-axis) versus the nearest neighbor internucleosomal distances (*x*-axis), are shown for hypoacetylated (upper panel) and highly acetylated (lower panel) MMTV arrays. The points are experimental values; the thick solid line is the theoretical (random) distribution of expected lengths. The dotted lines show the 3σ limit of statistical deviations from random. Experimental values beyond those limits are considered significant. Images were taken in solution.

Table 2: Virial Coefficients[a] and Energies[a] for Nearest Neighbor Nucleosome Interactions

array	histone state	virial coeff υ_2 (bp)	interaction energies V_2 (kcal M^{-1})
MMTV	hypoacetylated	25	−0.32
	hyperacetylated	−14	0.30
5S[b]	hypoacetylated	20	−0.25
	hyperacetylated	−10	0.15

[a] Uncertainties are ±10 bp for virial coefficients and ±0.15 kcal/M for interaction energies. [b] The 5S data are taken from Table 3 of ref *19*.

19). However, that peak is absent in distance plots for highly acetylated arrays (Figure 3, lower panel); in fact, for these arrays, very short internucleosomal distances are slightly underpopulated compared to a random expectation. Thus, the tendency for cooperative occupation is abolished in highly acetylated MMTV arrays.

This effect can be quantified using the model, by determining the values of the virial coefficients (see Materials and Methods) and thus the average interaction energies per pair of nucleosomes (calculated from the virial coefficients). These quantities are shown in Table 2 for hypo- and hyperacetylated MMTV (from this work) and 208-12 5S (from Table 3 of ref *19*) arrays. Hypoacetylated arrays of both types show a tendency for cooperative occupation that is abolished in highly acetylated arrays. However, the cooperative tendency is somewhat stronger in MMTV than in 5S hypoacetylated arrays, and the change is somewhat larger in the highly acetylated MMTV (vs 5S) arrays. The positive energy values (negative virial coefficients) observed with both types of highly acetylated arrays are probably due to steric (interference) effects (*19*).

Salt Stabilities. The repetitive solution imaging capabilities of AFM were used previously to study the salt stabilities of nucleosomes in hypoacetylated MMTV and 5S arrays (*26*, *27*). Here, salt stabilities of highly acetylated nucleosomes are characterized for both types of arrays. To carry out these studies, (subsaturated) nucleosomal arrays are deposited on GD-APTES mica, which tethers nucleosomes through the histones, and then imaged in a flow cell attached to the AFM. Surface tethering permits repeated scanning of the same group of individual array molecules (the same area of the surface) as salt solutions of increasing concentration are flowed into the cell. The resulting series of images over a range of salt concentrations tracks the progressive release of DNA from the nucleosomes (histones) in individual arrays, thus generating a single molecule level determination of nucleosome salt stability in arrays. This experiment is possible because, despite being tethered to the surface, both the DNA (*26*, *27*, *32*, *33*) and at least some histones (*34*) in these arrays maintain significant amounts of freedom.

Figure 4 (upper panel) shows examples of such salt "titrations" for three samples, two highly acetylated (filled circles) and one hypoacetylated (filled triangles). Samples are characterized by n_{av}, the average number of nucleosomes on the arrays in that sample. To take into account the inherent variation in nucleosome occupation levels within a sample, the fraction of nucleosomes in an array that have *not* released their DNA is plotted as a function of [NaCl]. This fraction is calculated as the number of nucleosomes present in an array at any [NaCl] divided by the number present on that nucleosomal array initially (at very low salt concentration). Whether judged by the mid-point (50% bound) or end-point (0% bound) values in such titrations, highly acetylated nucleosomes have a lower salt stability than hypoacetylated nucleosomes in MMTV arrays.

A very useful approach is to compile the titration data from all the individual sample titrations and group it by *n*, the specific number of nucleosomes in the array (Figure 4, lower panel). In this case, the average salt concentration required for nucleosomal DNA loss, i.e., the value averaged over all of the nucleosomes in an array containing *n* nucleosomes, is plotted versus *n*. Thus, nucleosomal DNA loss data from array molecules that contain $n = 2$ nucleosomes, $n = 3$ nucleosomes, etc. are separately displayed. Pooling the data in this way increases the numbers of molecules, thus enhancing the statistical accuracy, it provides an easy way to assess variance in the data, and, most importantly, it can reveal occupation level-dependent variations. Previously, we found that hypoacetylated nucleosome salt stabilities are greater in MMTV than in 5S arrays and that MMTV salt stabilities are occupation level-dependent at low occupation levels ($n < 4$) but 5S stabilities are remarkably constant over the whole range of occupation studied (Figure 6 of ref *27*).

The results in Figure 4 (lower panel) show several features:

(1) In agreement with the results shown in the upper panel of Figure 4, the presence of highly acetylated histones decreases the salt stabilities of nucleosomes in MMTV arrays, at least for occupation levels up to $n \sim 6$ (filled circles vs

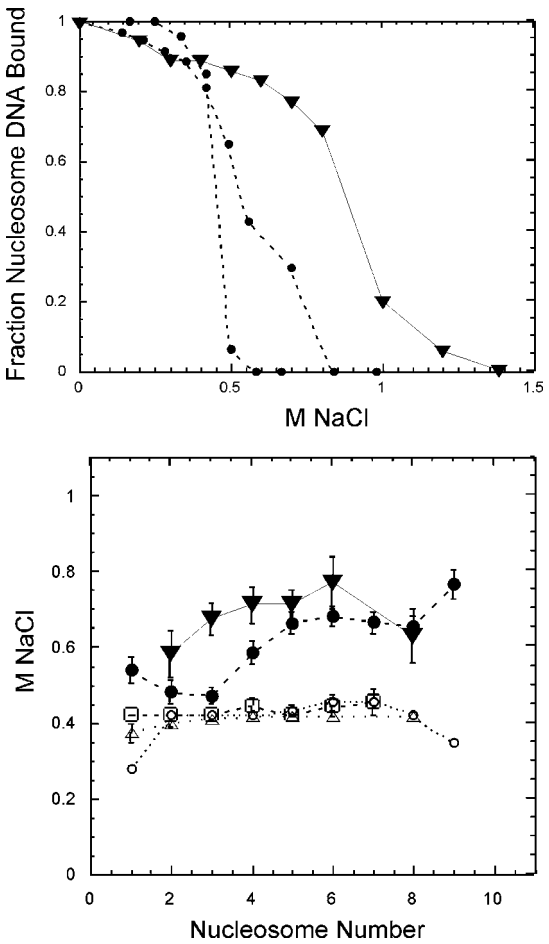

FIGURE 4: Acetylation decreases nucleosome salt stability in MMTV arrays. The upper panel shows plots of the fraction of nucleosomes that maintain their DNA, i.e., it has not been released from the histone core, versus [NaCl] for arrays in two highly acetylated MMTV samples (filled circles), $n_{av} = 4.7$ and $n_{av} = 6.5$, and one hypoacetylated sample (filled triangles), $n_{av} = 5.9$. The lower panel shows plots of the average NaCl concentration required for nucleosomal DNA loss (averaged over all of the nucleosomes in an array molecule) compiled from salt titration experiments such as those in the upper panel but collated by *n* class, i.e., by the total number of nucleosomes on an array (in low salt), and plotted versus *n*. These plots include data from all of the salt titrations that were done, across the spectrum of n_{av}. Data for highly acetylated MMTV (filled circles) and 172-12 (open triangles) as well as previously determined data (*27*) for hypoacetylated MMTV (filled triangles), hypoacetylated 172-12 (open squares), and hypoacetylated 208-12 (open circles) 5S arrays are also shown. The lines connect the data points and are simply present to aid in visualization. Imaging was carried out in solution.

filled triangles). In contrast, there is no effect on 5S nucleosome salt stabilities at any occupation level; hyper- and hypoacetylated nucleosome stabilities in 5S arrays are the same across the whole range of occupation studied here (open triangles vs open squares).

(2) The salt stabilities of highly acetylated MMTV nucleosomes show occupation level dependence at the lower occupation levels ($n \leq 5$), as do hypoacetylated MMTV nucleosomes. 5S nucleosomes, hyper- or hypoacetylated, show no occupation level dependence of stability (open triangles vs open squares or circles).

(3) The stabilities of highly acetylated MMTV nucleosomes remain higher than the stabilities of 5S nucleosomes. The two are closest at very low occupation levels ($n < 4$).

As discussed at length in ref *27* and below, the presence and/or interaction of the surface with the arrays could affect nucleosome salt stability. For example, less extensive attachment of highly acetylated arrays to the surface (see above) could contribute to lowering salt stabilities. However, these surface influences should affect both 5S and MMTV arrays similarly since the two types of arrays contain the same histones. Thus, template-associated acetylation differences, namely, that the presence of highly acetylated histones lowers MMTV but not 5S stabilities and that stabilities for highly acetylated MMTV nucleosomes can vary with occupation level but 5S do not, must reflect differences that are due to the different DNA templates in the two types of arrays. Thus, acetylation effects on the salt stability of nucleosomes in arrays can vary with DNA template.

In previous work with hypoacetylated MMTV arrays, it was suggested that the observed dropoff in stability at $n > 6$ (cf. Figure 4 lower panel, filled triangles) could reflect a decreased ability to accommodate the torsional stress generated by DNA release from nucleosomes as arrays become increasingly nucleosome-occupied. That this does not occur with highly acetylated arrays, at least up to $n = 9$ (filled circles), is consistent with the suggested lower level of restrained supercoiling in individual acetylated nucleosomes (reviewed in ref *3*) because each nucleosomal length of DNA released in acetylated arrays would release less torsion. The small shift in the range where occupation level dependence is observed ($n = 2-4$ for hypoacetylated vs $n = 3-5$ for hyperacetylated arrays) could also be due to decreased DNA restraint in acetylated nucleosomes.

We note one other feature that these results indicate regarding nucleosome salt stability. Titrations like those shown in the upper panel of Figure 4 are broadest for acetylated MMTV samples with average occupation levels $\cong$6, which corresponds to 50% of saturation on this MMTV template (*27*). For example, whereas the curve for the $n_{av} = 4.7$ highly acetylated sample is fairly sharp, with 80% of the change (from 90% to 10%) occurring within a range of $\sim$0.15 M in [salt], the curve for the $n_{av} = 6.5$ acetylated sample is much broader; 80% of the change occurs over a range $>$0.5 M in [salt]. Hypoacetylated MMTV samples show similar behavior (*27*). Broadening reflects a greater heterogeneity in these mid-occupation range samples. On the other hand, 5S transitions are sharp (80% change requiring $<$0.2 M change in [salt]), at all occupation levels, in hypoacetylated (*27*) as well as hyperacetylated samples (data not shown). Thus, an enhanced breadth in midrange samples is another MMTV vs 5S behavioral difference. Acetylation is obligatory for assembly of newly synthesized histones into chromatin (*49*). If subsaturated, acetylated MMTV arrays can be considered a model for replicating chromatin, then these data would suggest that $\sim$50% array occupation levels offer the greatest inherent opportunities for variations in nucleosome stabilities and thus possibly in occupation patterns. This property could play a role in vivo in the assembly of the variety of chromatin structures that need to be established during replication.

Nucleosome Remodeling of Highly Acetylated Arrays. Previously, we used AFM techniques to study the basic features of nucleosome remodeling of hypoacetylated MMTV arrays by the ATP-dependent nucleosome remodeling complex, human Swi-Snf (*32*). The approach involves imaging

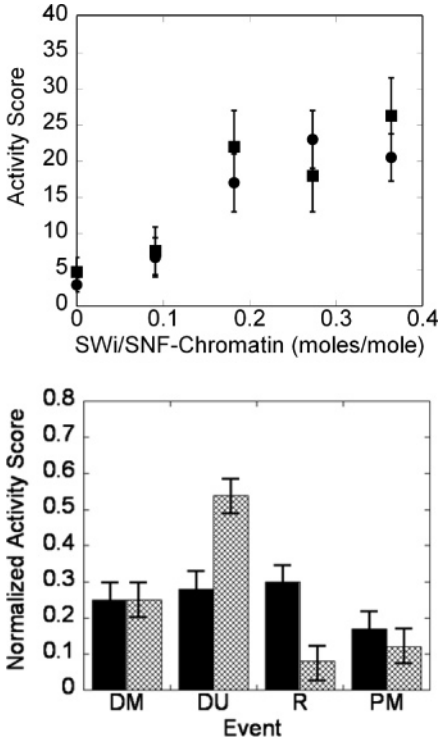

FIGURE 5: hSwi-Snf remodeling of highly acetylated and hypoacetylated MMTV arrays. The upper panel shows a dose response curve, activity score versus the ratio of hSwi-Snf:chromatin molecules. Activity score reflects the number of remodeling changes; it is the number of nucleosomes that have undergone change (+ATP compare to −ATP) divided by the total number of chromatin molecules present in the image field (see also ref *32*). Squares show results for highly acetylated arrays, and circles show results for hypoacetylated arrays. The lower panel shows normalized frequencies for the various types of remodeling events (see text) for highly acetylated MMTV arrays (hatched bars) or hypoacetylated arrays (solid bars; from ref *32*).

the same individual array molecules before and after activation of remodeling by addition of ATP to hSwi-Snf/MMTV chromatin samples deposited in situ in a flow cell linked to the AFM. In that study, we analyzed the "dose response", i.e., the frequency of remodeling events as a function of hSwi-Snf levels, and divided the observed remodeling events into four basic classes (*32*): (i) "DNA movement" (DM) or "protein movement" (PM) events, which involve relocation of preexisting DNA segments or protein particles (including the appearance of new particles on DNA) after ATP addition; (ii) "DNA unwrapping" (DU) events, which involve new DNA appearing at the former location of a nucleosomal or subnucleosomal particle or the extrusion of DNA from very large particles that are probably hSwi-Snf and/or aggregated chromatin after ATP addition; (iii) "rewiring" events (R), which involve major changes in the DNA path in arrays after ATP addition. Only the first two classes of events, DNA and protein movements, are observed in repetitive scans of hSwi-Snf/MMTV chromatin samples carried out in the absence of ATP, which is a control to assess instrument-induced changes (*32*). Thus, the other two types of events are clearly remodeling-associated.

Here, we carry out a similar analysis of hSwi-Snf remodeling of MMTV arrays containing highly acetylated histones. We find that the dose response of highly acetylated and hypoacetylated arrays is similar (Figure 5, upper panel). To analyze the event frequency in highly acetylated chromatin, a total of 103 local areas showing remodeling changes were chosen and analyzed in detail. Those areas sometimes contained multiple molecules and could therefore show multiple types of changes. Highly acetylated arrays show the same basic types of remodeling events as hypoacetylated arrays (Figure 5, lower panel). As was the case for hypoacetylated arrays (*32*), DU and rewiring of acetylated arrays are remodeling-specific events; those events are not observed in repetitive scans of samples (MMTV arrays plus hSwi-Snf) carried out in the absence of ATP (Wang et al., unpublished results).

The relative proportions of DM and PM events are similar in highly acetylated or hypoacetylated samples (Figure 5, lower panel). However, the remodeling-specific events, DU and R events, differ somewhat in relative frequency; the proportion of rewiring events is lower and the proportion of DU events is higher for highly acetylated samples. Rewiring events are the most dramatic type of remodeling change. That they are less common in the hyperacetylated data set is consistent with our general impression that remodeling changes on acetylated MMTV arrays are, if anything, less robust than the changes we observe on hypoacetylated arrays (*32*). This was true even in remodeling experiments done the same day, with the same hSwi-Snf etc. However, differential remodeling activity is difficult to establish firmly because hSwi-Snf activity could vary from deposition to deposition. Highly acetylated arrays may be less firmly tethered to the surface than hypoacetylated arrays. However, that difference should enhance remodeling of the highly acetylated arrays, which is not the case. Other kinds of results have indicated only a modest role for histone tails in hSwi-Snf nucleosome remodeling activities (*59*), which is consistent with the absence of significant differences in hSwi-Snf remodeling of hyper- and hypoacetylated MMTV arrays.

Some specific examples of DU and R events observed with highly acetylated arrays are shown in Figure 6. Yellow arrowheads in the −ATP image mark the sites where changes will occur, and the changes are located by green arrowheads in the +ATP image. We characterize particles as nucleosomes or subnucleosomal particles (cf. H3/H4 tetramer−DNA complexes) in these images based on their heights, using previously determined criteria (*33*, *34*; Bash et al., unpublished results). Also, several hSwi-Snf complexes were located in these images (blue arrows in Figure 6, panels A and B), again based on previously determined criteria, heights >4.2 nm, widths 45−70 nm (*33*). Remodeling events often occur in the proximity of such complexes.

In panels A, an H3/H4 tetramer−DNA sized particle ("1", −ATP image) and a nucleosome-sized particle ("2", −ATP image) have disappeared after ATP addition, releasing 25 nm and an undeterminable amount (due to path uncertainties) of DNA, respectively. In the lower portion of panels A, two smaller particles ("3" in −ATP image) have coalesced into a larger one after ATP addition (an uncommon event) and an H3/H4 tetramer-sized particle ("4" in −ATP image) lying next to a hSwi-Snf complex (blue arrow in −ATP image) has disappeared, releasing 25 nm of DNA. Particles with heights characteristic of H3/H4 tetramer−DNA complexes are common in these images, and hSwi-Snf complexes often are found lying close to them and to one another (Figure 6 A, blue arrows, −ATP image). Both features are also commonly observed in samples of hypoacetylated arrays plus

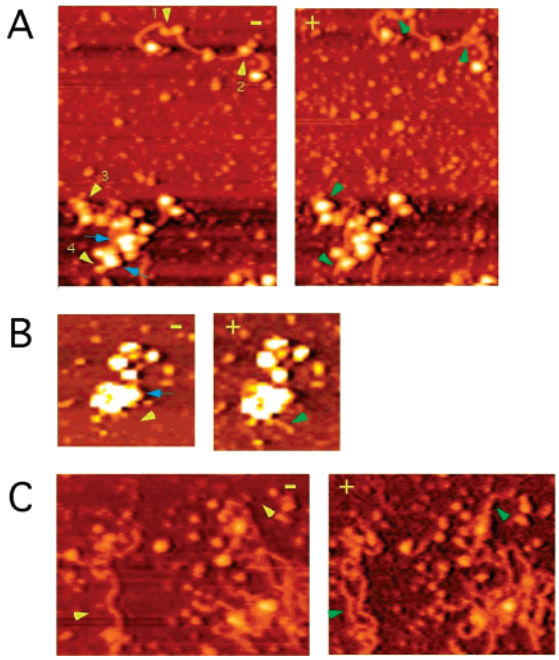

FIGURE 6: Examples of nucleosome remodeling of acetylated MMTV arrays. These pairs of images (A−C) show the same array molecules before (−) and after (+) ATP addition (to activate hSwi-Snf). Sites where changes will occur are identified by yellow arrowheads in the −ATP panel, and the changes are marked by green arrowheads in the corresponding +ATP panel. The blue arrows identify hSwi-Snf molecules, based on criteria in ref *33*, heights ≥4.2 nm and widths >40 nm. Note that the two terminal particles on the upper molecule in panel A (containing events 1 and 2) are taller than typical nucleosomes but fall below the unambiguous hSwi-Snf criteria; they could be partially dissociated hSwi-Snf complexes, which are common in images of hSwi-Snf (*33*). These smaller complexes typically contain the ATPase subunit, BRG1, and thus can still remodel chromatin. Imaging was carried out in solution. The same types of events for hypoacetylated chromatin have been described in greater detail in ref *33*.

hSwi-Snf (*33*). In panels B, another very common remodeling change is shown, extrusion of DNA, ∼40 nm (green arrowhead), from under a hSwi-Snf-sized complex (blue arrow) after ATP addition. Some DNA (∼45 nm) is also extruded near the top of this complex. In panels C, rewiring changes, i.e., major alterations in DNA path, are observed after ATP addition (green arrowheads, +ATP image), involving the appearance of ∼100 nm (upper right green arrow) and ∼150 nm (lower left green arrow) of DNA, respectively.

DISCUSSION

Using AFM approaches, we have characterized the properties of MMTV promoter nucleosomal arrays reconstituted with highly acetylated histones (isolated from butyrate-treated HeLa cells; see Materials and Methods) and compared their properties to those of hypoacetylated MMTV and hyper- and hypoacetylated 5S rDNA arrays. The two most significant effects noted when these highly acetylated histones are present in MMTV arrays are (1) mitigation of the compaction that occurs at subsaturated occupation levels (Figure 1) and (2) loss of cooperativity in nucleosome occupation (Figure 3), both of which are prominent features of hypoacetylated MMTV arrays. Qualitatively similar results are found for hyper- vs hypoacetylated 5S arrays (*18*, *19*), but there are some quantitative differences (see below).

The presence of these highly acetylated histones also results in some qualitative behavioral differences between MMTV and 5S arrays. In MMTV arrays, nucleosome salt stability is lowered (at low to mid levels of array occupation) in highly acetylated vs hypoacetylated arrays (Figure 4), but the thermodynamic tendencies for nucleosome (histone) loading on the MMTV DNA template are unaffected by the use of acetylated histones (Figure 2), as measured by nucleosome association constants (Table 1). In contrast, loading tendencies on 5S arrays are reduced somewhat when using highly acetylated histones (*19*, *20*; Table 1), but nucleosome salt stability is unaffected (Figure 4). Thus, the effects produced by the presence of acetylated nucleosomes in arrays can vary, either qualitatively or quantitatively, with the nature of the DNA template. Since the same sets of highly acetylated and hypoacetylated histones are used to reconstitute both types of arrays, these differences must reflect DNA template-dependent features.

The use of the deacetylase inhibitor sodium butyrate to isolate histones with high levels of acetylation (*60*, *61*) has been employed extensively in studies of the effects of acetylation on chromatin. In such histone preparations, the N-terminal histone tails are typically highly acetylated, and this is known to diminish the ability of the tails to mediate internucleosomal interactions (*6*, *11*). Therefore, array properties that involve significant levels of tail-mediated internucleosomal contacts should be significantly affected by the presence of these histones, and this is the case in our studies. Compaction, the AFM analogue of chromatin folding in solution (*27*), and cooperative nucleosome occupation both depend strongly on tail-mediated internucleosomal interactions, and as noted above, both are significantly affected by the presence of these highly acetylated histones. The levels of both H4 Lys_{16} acetylation, which strongly affects solution chromatin folding (*54*), and core domain acetylation, which could also affect compaction (reviewed in ref *48*), are unknown in our acetylated histone preparations. Thus, it is possible that compaction differences (and perhaps cooperativity differences) between highly acetylated and hypoacetylated arrays (MMTV or 5S) could be stronger than those we observe. Also, other histone modifications (methylation, phosphorylation) can be present in histones from butyrate-treated cells; the possible effects of these modifications are currently impossible to evaluate. However, while specific histone features (H4 Lys_{16} or core acetylation or other types of modifications) could affect the magnitude of the observed highly acetylated vs hypoacetylated differences, they cannot alter the conclusion that there are DNA template-dependent differences between 5S and MMTV since the same sets of histones were used to make both types of highly acetylated and hypoacetylated arrays.

The template-dependent differences in nucleosome salt stability (Figure 4) are harder to explain. Nucleosome salt stabilities ought to reflect, at least in part, the inherent strength of the histone octamer−DNA interaction. We show here that 5S DNA, one of the strongest known natural histone binding sequences in mononucleosome studies (*62*, *63*), binds histones more strongly than MMTV DNA, by at least 10-fold on a per nucleosome basis (Table 1). Yet the salt stability

of MMTV nucleosomes in arrays is significantly higher than that of 5S nucleosomes. It was argued in ref *27* that other effects besides the inherent strength of the DNA−histone interaction could affect the salt stability of nucleosomes in arrays, for example, "higher order" effects such as internucleosomal interactions and DNA torsional or topological constraints. The variation of salt stability with number of nucleosomes in hypoacetylated MMTV arrays and the sensitivity of this response to the presence of acetylated histones (Figure 4) both argue for the involvement of internucleosomal (higher order) effects in determining nucleosome salt stability in MMTV arrays. The enhanced cooperativity (Table 2) and enhanced compaction of hypoacetylated MMTV vs 5S arrays suggest that tail-mediated internucleosomal contacts may play a more significant role in (subsaturated) MMTV than 5S arrays, and this difference could contribute to the enhanced MMTV nucleosome stability. However, these differences seem too modest to account completely for the substantial salt stability differences observed between hypoacetylated MMTV and 5S nucleosomes in arrays (Figure 4). Also, in acetylated MMTV arrays, the levels of internucleosomal contacts are greatly reduced (Figure 3), but these nucleosomes maintain a higher salt stability than even hypoacetylated 5S nucleosomes, at least for occupation levels $n \geq 5$. Thus, other effects are probably involved. For example, if there is acetylation of residues within the histone core domain, which can affect DNA−histone contacts (*48*), this could contribute to the salt stability differences, but to account for these differences, the contributions would have to be DNA template-dependent. The reduced positive charge of acetyated tails might contribute to the reduced salt stability of acetylated MMTV nucleosomes, but why 5S nucleosome stabilities are unaffected is unclear.

In our studies, arrays are physically tethered to a surface, which has some obvious consequences for these arguments. For example, surface attachment has the potential to enhance the strength of the topological boundaries that nucleosomes themselves can create (*64*), thus magnifying small template-dependent differences arising from such constraints. Whether this would have a stabilizing (for MMTV) or destabilizing (for 5S) effect on salt stability is unclear. Second, since nucleosomes are tethered to the surface through lysines, probably in the tails, highly acetylated arrays may be less firmly attached to the surface than hypoacetylated arrays. However, it seems unlikely that this or any other surface effect would be DNA template-dependent since the histone component is mainly involved in the interactions with the surface and the same sets of histones were used to reconstitute the two templates.

5S and MMTV arrays differ in intrinsic DNA sequence and in template organization; 5S is repetitive whereas MMTV is single copy. Both features could contribute to the differences noted between the two. For example, nucleosome association constant differences between MMTV and 5S are probably DNA sequence features. On the other hand, template organization differences could help to reduce the role of internucleosomal contacts in 5S arrays, by tempering nearest neighbor contacts due to the strong positioning preference of the 5S units in the 208-12 template and their relatively large separation, compared to MMTV arrays, in which positioning is weaker and nucleosomes are freer to locate next to one another (discussed further in ref *27*). 5S arrays are commonly used as a model for chromatin behavior in vivo, but the results in this work suggest that 5S arrays have properties that differ from the typical (in vivo) single copy arrays. Thus, the MMTV array may be a more appropriate model. For example, on the basis of the compaction differences observed between MMTV and 5S arrays, 5S arrays may underestimate the extent of folding of in vivo arrays.

The observation of differential responses to the presence of acetylated histones in 5S vs MMTV arrays indicates that acetylation effects can be DNA template- and/or DNA sequence-dependent. Histones are known to bind with differing thermodynamic affinities on different DNA sequences (*56*, *62*, *63*, *65*), as we observe, and the stability and dynamics of DNA−histone association can also vary with DNA sequence (*65*−*67*). Other DNA sequence-dependent behaviors include nucleosome repositioning tendencies and remodeling (*68*, *69*), nucleosome mechanical stability (*70*), ligand−nucleosomal DNA interactions (*71*, *72*), and the roles of histone tails in nucleosome stability (*73*), which is consistent with our observation of sequence-dependent acetylation effects. To this list of sequence-dependent features, we would add the effects of acetylation on occupational cooperativity, loading tendencies, and salt stabilities of nucleosomes in arrays.

REFERENCES

1. Widom, J. (1998) Structure, dynamics, and function of chromatin in vitro, *Annu. Rev. Biophys. Biomol. Struct. 27*, 285−327.
2. Workman, J. L., and Kingston, R. E. (1998) Alteration of nucleosome structure as a mechanism of transcriptional regulation, *Annu. Rev. Biochem. 67*, 545−579.
3. Wolffe, A. P., and Hayes, J. J. (1999) Chromatin disruption and modification, *Nucleic Acids Res. 27*, 711−720.
4. Wolffe, A. P., and Guschin, D. (2000) Chromatin structural features and targets that regulate transcription, *J. Struct. Biol. 129*, 102−122.
5. Hayes, J. J., and Hansen, J. C. (2001) Nucleosomes and the chromatin fiber, *Curr. Opin. Genet. Dev. 11*, 124−129.
6. Hansen, J. C. (2002) Conformational dynamics of the chromatin fiber in solution: Determinants, mechanisms, and functions, *Annu. Rev. Biophys. Biomol. Struct. 31*, 361−392.
7. Luger, K. (2003) Structure and dynamic behavior of nucleosomes, *Curr. Opin. Genet. Dev. 13*, 127−135.
8. Luger, K., and Hansen, J. C. (2005) Nucleosome and chromatin fiber dynamics, *Curr. Opin. Struct. Biol. 15*, 188−196.
9. Woodcock, C. L. (2006) Chromatin architecture, *Curr. Opin. Struct. Biol. 16*, 213−220.
10. Fletcher, T. M., and Hansen, J. C. (1996) The nucleosomal array: Structure/function relationships, *Crit. Rev. Eukaryotic Gene Expression 6*, 149−188.
11. Hansen, J. C., Tse, C., and Wolffe, A. P. (1998) Structure and function of the core histone N-termini: More than meets the eye, *Biochemistry 37*, 17637−17641.
12. Simpson, R. T., Thoma, F., and Brubaker, J. M. (1985) Chromatin reconstituted from tandemly repeated cloned DNA fragments and core histones−a model system for study of higher-order structure, *Cell 42*, 799−808.
13. Carruthers, L. M., Tse, C., Walker, K. P., and Hansen, J. C. (1999) Assembly of defined nucleosomal and chromatin arrays from pure components, *Chromatin 304*, 19−35.
14. Dong, F., Hansen, J. C., and Vanholde, K. E. (1990) DNA and protein determinants of nucleosome positioning on sea-urchin 5S ribosomal-RNA gene-sequences in vitro, *Proc. Natl. Acad. Sci. U.S.A. 87*, 5724−5728.
15. Meersseman, G., Pennings, S., and Bradbury, E. M. (1991) Chromatosome positioning on assembled long chromatin linker histones affect nucleosome placement on 5-S-rDNA, *J. Mol. Biol. 220*, 89−100.

16. Hansen, J. C., Vanholde, K. E., and Lohr, D. (1991) The mechanism of nucleosome assembly onto oligomers of the sea-urchin 5-S DNA positioning sequence, *J. Biol. Chem. 266*, 4276−4282.
17. Yodh, J. G., Lyubchenko, Y. L., Shlyakhtenko, L. S., Woodbury, N., and Lohr, D. (1999) Evidence for nonrandom behavior in 208-12 subsaturated nucleosomal array populations analyzed by AFM, *Biochemistry 38*, 15756−15763.
18. Yodh, J. G., Woodbury, N., Shlyakhtenko, L. S., Lyubchenko, Y. L., and Lohr, D. (2002) Mapping nucleosome locations on the 208-12 by AFM provides clear evidence for cooperativity in array occupation, *Biochemistry 41*, 3565−3574.
19. Solis, F. J., Bash, R., Yodh, J., Lindsay, S. M., and Lohr, D. (2004) A statistical thermodynamic model applied to experimental afm population and location data is able to quantify DNA-histone binding strength and internucleosomal interaction differences between acetylated and hypoacetylated nucleosomal arrays, *Biophys. J. 87*, 3372−3387.
20. Bash, R. C., Yodh, J., Lyubchenko, Y., Woodbury, N., and Lohr, D. (2001) Population analysis of subsaturated 172-12 nucleosomal arrays by atomic force microscopy detects nonrandom behavior that is favored by histone acetylation and short repeat length, *J. Biol. Chem. 276*, 48362−48370.
21. Lyubchenko, Y. L., Jacobs, B. L., Lindsay, S. M., and Stasiak, A. (1995) Atomic-force microscopy of nucleoprotein complexes, *Scanning Microsc. 9*, 705−727.
22. Lindsay, S. M. (2000) The scanning probe microscope in biology, in *Scanning probe microscopy and spectroscopy: Theory, techniques, and applications* (Bonnell, D., Ed.) Wiley-VCH, New York.
23. Hansma, H. G., Kasuya, K., and Oroudjev, E. (2004) Atomic force microscopy imaging and pulling of nucleic acids, *Curr. Opin. Struct. Biol. 14*, 380−385.
24. Sato, M. H., Ura, K., Hohmura, K. I., Tokumasu, F., Yoshimura, S. H., Hanaoka, F., and Takeyasu, K. (1999) Atomic force microscopy sees nucleosome positioning and histone H1-induced compaction in reconstituted chromatin, *FEBS Lett. 452*, 267−271.
25. Schnitzler, G. R., Cheung, C. L., Hafner, J. H., Saurin, A. J., Kingston, R. E., and Lieber, C. M. (2001) Direct imaging of human swi/snf-remodeled mono- and polynucleosomes by atomic force microscopy employing carbon nanotube tips, *Mol. Cell. Biol. 21*, 8504−8511.
26. Wang, H. D., Bash, R., Yodh, J. G., Hager, G. L., Lohr, D., and Lindsay, S. M. (2002) Glutaraldehyde modified mica: A new surface for atomic force microscopy of chromatin, *Biophys. J. 83*, 3619−3625.
27. Bash, R., Wang, H., Yodh, J., Hager, G., Lindsay, S. M., and Lohr, D. (2003) Nucleosomal arrays can be salt-reconstituted on a single-copy mmtv promoter DNA template: Their properties differ in several ways from those of comparable 5S concatameric arrays, *Biochemistry 42*, 4681−4690.
28. Nikova, D. N., Pope, L. H., Bennink, M. L., van Leijenhorst-Groener, K. A., van der Werf, K., and Greve, J. (2004) Unexpected binding motifs for subnucleosomal particles revealed by atomic force microscopy, *Biophys. J. 87*, 4135−4145.
29. Lohr, D. (1997) Nucleosome transactions on the promoters of the yeast gal and pho genes, *J. Biol. Chem. 272*, 26795−26798.
30. Sogo, J. M., Stahl, H., Koller, T., and Knippers, R. (1986) Structure of replicating simian virus-40 minichromosomes—the replication fork, core histone segregation and terminal structures, *J. Mol. Biol. 189*, 189−204.
31. Lohr, D., and Torchia, T. (1988) Structure of the chromosomal copy of yeast ars1, *Biochemistry 27*, 3961−3965.
32. Wang, H., Bash, R., Yodh, J. G., Hager, G., Lindsay, S. M., and Lohr, D. (2004) Using atomic force microscopy to study nucleosome remodeling on individual nucleosomal arrays in situ, *Biophys. J. 87*, 1964−1971.
33. Wang, H., Bash, R., Lindsay, S. M., and Lohr, D. (2005) Solution AFM studies of human Swi-Snf and its interactions with MMTV DNA and chromatin, *Biophys. J. 89*, 3386−3398.
34. Bash, R., Wang, H., Anderson, C., Yodh, J., Hager, G., Lindsay, S. M., and Lohr, D. (2006) Afm imaging of protein movements: Histone H2a-H2b release during nucleosome remodeling, *FEBS Lett. 580*, 4757−4761.
35. Stroh, C., Wang, H., Bash, R., Ashcroft, B., Nelson, J., Gruber, H., Lohr, D., Lindsay, S. M., and Hinterdorfer, P. (2004) Single-molecule recognition imaging-microscopy, *Proc. Natl. Acad. Sci. U.S.A. 101*, 12503−12507.
36. Hager, G., Smith, C., Svaren, J., and Horz, W. (1994) Initiation of expression: Remodelling genes, in *Chromatin structure and gene expression* (Elgin, S. C. R., Ed.) pp 89−103, Oxford University Press, Oxford.
37. Hager, G. L. (2001) Understanding nuclear receptor function: From DNA to chromatin to the interphase nucleus, *Prog. Nucleic Acid Res. Mol. Biol. 66*, 279−305.
38. Fletcher, T. M., Ryu, B. W., Baumann, C. T., Warren, B. S., Fragoso, G., John, S., and Hager, G. L. (2000) Structure and dynamic properties of a glucocorticoid receptor-induced chromatin transition, *Mol. Cell. Biol. 20*, 6466−6475.
39. Fletcher, T. M., Xiao, N. Q., Mautino, G., Baumann, C. T., Wolford, R., Warren, B. S., and Hager, G. L. (2002) ATP-dependent mobilization of the glucocorticoid receptor during chromatin remodeling, *Mol. Cell. Biol. 22*, 3255−3263.
40. Strahl, B. D., and Allis, C. D. (2000) The language of covalent histone modifications, *Nature 403*, 41−45.
41. Berger, S. L. (2002) Histone modifications in transcriptional regulation, *Curr. Opin. Genet. Dev. 12*, 142−148.
42. Turner, B. M. (2002) Cellular memory and the histone code, *Cell 111*, 285−291.
43. Fischle, W., Wang, Y. M., and Allis, C. D. (2003) Histone and chromatin cross-talk, *Curr. Opin. Cell Biol. 15*, 172−183.
44. Iizuka, M., and Smith, M. M. (2003) Functional consequences of histone modifications, *Curr. Opin. Genet. Dev. 13*, 154−160.
45. Khorasanizadeh, S. (2004) The nucleosome: From genomic organization to genomic regulation, *Cell 116*, 259−272.
46. Peterson, C. L., and Laniel, M. A. (2004) Histones and histone modifications, *Curr. Biol. 14*, R546−R551.
47. de la Cruz, X., Lois, S., Sanchez-Molina, S., and Martinez-Balbas, M. A. (2005) Do protein motifs read the histone code?, *BioEssays 27*, 164−175.
48. Cosgrove, M., Boeke, J., and Wolberger, C. (2004) Regulated nucleosome mobility and the histone code, *Nat. Struct. Mol. Biol. 11*, 1037−1043.
49. Annunziato, A. T., and Hansen, J. C. (2000) Role of histone acetylation in the assembly and modulation of chromatin structures, *Gene Expression 9*, 37−61.
50. Grunstein, M. (1997) Histone acetylation in chromatin structure and transcription, *Nature 389*, 349−352.
51. Horn, P. J., and Peterson, C. L. (2002) Molecular biology: Chromatin higher order folding: Wrapping up transcription, *Science 297*, 1824−1827.
52. Narlikar, G. J., Fan, H. Y., and Kingston, R. E. (2002) Cooperation between complexes that regulate chromatin structure and transcription, *Cell 108*, 475−487.
53. Garcia-Ramirez, M., Rocchini, C., and Ausio, J. (1995) Modulation of chromatin folding by histone acetylation, *J. Biol. Chem. 270*, 17923−17928.
54. Shogren-Knaak, M., Ishii, H., Sun, J. M., Pazin, M. J., Davie, J. R., and Peterson, C. L. (2006) Histone H4-K16 acetylation controls chromatin structure and protein interactions, *Science 311*, 844−847.
55. VanHolde, K., and Zlatanova, J. (1999) The nucleosome core particle: does it have physiological relevance?, *BioEssays 21*, 776−780.
56. Wu, C. Y., and Travers, A. (2005) Relative affinities of DNA sequences for the histone octamer depend strongly upon both the temperature and octamer concentration, *Biochemistry 44*, 14329−14334.
57. Flaus, A., and Richmond, T. J. (1998) Positioning and stability of nucleosomes on MMTV 3′ LTR sequences, *J. Mol. Biol. 275*, 427−441.
58. Neubauer, B., and Horz, W. (1989) Analysis of nucleosome positioning by in vitro reconstitution, *Methods Enzymol. 170*, 630−644.
59. Guyon, J. R., Narlikar, G. J., Sif, S., and Kingston, R. E. (1999) Stable remodeling of tailless nucleosomes by the human Swi-Snf complex, *Mol. Cell. Biol. 19*, 2088−2097.
60. Candido, P., Reeves, R., and Davie, J. R. (1978) Sodium butyrate inhibits histone deacetylation in cultured cells, *Cell 14*, 105−113.
61. Sealy, L., and Chalkley, R. (1978) The effect of sodium butyrate on histone modification, Cell *14*, 115−121.
62. Shrader, T. E., and Crothers, D. M. (1989) Artificial nucleosome positioning sequences, *Proc. Natl. Acad. Sci. U.S.A. 86*, 7418−7422.

63. Thastrom, A., Lowary, P. T., Widlund, H. R., Cao, H., Kubista, M., and Widom, J. (1999) Sequence motifs and free energies of selected natural and non-natural nucleosome positioning DNA sequences, *J. Mol. Biol. 288*, 213−229.
64. Mondal, N., and Parvin, J. D. (2001) DNA topoisomerase IIa is required for RNA polymerase II transcription on chromatin templates, *Nature 413*, 435−438.
65. Widom, J. (2001) Role of DNA sequence in nucleosome stability and dynamics, *Q. Rev. Biophys. 34*, 269−324.
66. Kelbauskas, L., Chan, N., Bash, R., Yodh, J., Woodbury, N., and Lohr, D. (2007) Sequence-dependent nuclesome structure and stability variations detected by Forster resonance energy transfer, *Biochemistry 46*, 2239−2248.
67. Anderson, J. D., and Widom, J. (2000) Sequence and position-dependence of the equilibrium accessibility of nucleosomal DNA target sites, *J. Mol. Biol. 296*, 979−987.
68. Krajewski, W. A. (2002) Histone acetylation status and DNA sequence modulate ATP-dependent nucleosome repositioning, *J. Biol. Chem. 277*, 14509−14513.
69. Vicent, G. P., Nacht, A. S., Smith, C. L., Peterson, C. L., Dimitrov, S., and Beato, M. (2004) DNA instructed displacement of histories H2a and H2b at an inducible promoter, *Mol. Cell 16*, 439−452.
70. Gemmen, G. J., Sim, R., Haushalter, K. A., Ke, P. C., Kadonaga, J. T., and Smith, D. E. (2005) Forced unraveling of nucleosomes assembled on heterogeneous DNA using core, histones, NAP-1, and ACF, *J. Mol. Biol. 351*, 89−99.
71. Gottesfeld, J. M., Melander, C., Suto, R. K., Raviol, H., Luger, K., and Dervan, P. B. (2001) Sequence-specific recognition of DNA in the nucleosome by pyrrole-imidazole polyamides, *J. Mol. Biol. 309*, 615−629.
72. Babendure, J., Liddell, P. A., Bash, R., LoVullo, D., Schiefer, T. K., Williams, M., Daniel, D. C., Thompson, M., Taguchi, A. K. W., Lohr, D., and Woodbury, N. W. (2003) Development of a fluorescent probe for the study of nucleosome assembly and dynamics, *Anal. Biochem. 317*, 1−11.
73. Widlund, H. R., Vitolo, J. M., Thiriet, C., and Hayes, J. J. (2000) DNA sequence-dependent contributions of core histone tails to nucleosome stability: Differential effects of acetylation and proteolytic tail removal, *Biochemistry 39*, 3835−3841.

BI062116Z